JPL NO. 9950 - 666

E83-10172
CR-169782

Final Report

Evaluation of Seasat-A SMMR Derived Wind Speed Measurements

Prepared for

Jet Propulsion Laboratory
California Institute of Technology
Pasadena, California

Contract No. 955583

by

Oceanweather Inc.
170 Hamilton Avenue
White Plains, New York 10601

January, 1982

(E83-10172) EVALUATION OF SEASAT-A SMMR DERIVED WIND SPEED MEASUREMENTS Final Report (Oceanweather, Inc.) 41 p
HC A03/MF A01 CSCL 04B G3/43

N83-17936
Unclas
00172

Table of Contents

Introduction

The first geophysical data from SMMR were processed in late 1978 and were evaluated in the GOASEX workshop (January, 1979). Wind speed data derived from the SMMR were evaluated on the basis of detailed studies of data from four orbits (revs 1135, 1212, 1292, 1298) which covered a wide range of wind speeds and atmospheric conditions over the eastern North Pacific. Surface truth wind data for the four revs were derived by kinematic analysis of conventional data. Brown et al., 1982. Considering the immaturity of the interim geophysical algorithms applied, the comparisons were quite encouraging. Both the least square algorithm developed by Wentz and the regression algorithm developed by Wilheit tracked relative changes in the wind speeds observed, although both algorighms exhibited significant bias. (Lipes et al., 1979). The comparisons also revealed obvious deficiencies. In particular, the algorithms failed to provide reasonable absolute or relative measures of wind speed when rain was present. Also, unrealistic variation in bias with cross track position appeared in the preliminary wind statistics. Nevertheless, the early comparisons strongly suggested that the design accuracy of ±2 m/sec in wind speed determination could eventually be demonstrated from the SMMR data.

The algorithms were improved for the geophysical data processed for the SMMR Mini-Workshop (May, 1979) in several ways. First, sidelobe corrections were included in the antenna pattern correction (APC) algorithm to increase resolution of geophysical features. Second, a simple empirical procedure was employed to remove the cross-track gradients in brightness temperature (T_B) evident in the SMMR data. Changes were also made to correct known deficiencies in the antenna temperature algorithms. Finally, an attempt was made to calibrate the brightness temperatures in each SMMR channel in order to remove the discrepancies which existed between T_B's computed by the APC and T_B's computed by the Wentz geophysical function using surface truth estimates.

SMMR winds were compared with surface truth kinematic fields as well as with a small number of buoy and weather ship reports. The field comparisons showed the least-squares algorithm winds to exhibit a standard deviation of 2.3 m/sec about a 1 m/s positive bias with a tendency to overestimate low wind speeds. The regression algorithm showed a 2.8 m/s standard deviation about a 12.5 m/s positive bias. For the small number of revs processed for this workshop only 17 comparisons at buoy or weather ship locations were available. The comparisons with those spot reports were comparable in accuracy to the field comparisons.

The SMMR Mini-Workshop II of September 1979 examined a much larger number of revs in order to increase the number of comparisons at buoys and weather ships. Further improvements had been made in the APC and the antenna temperature algorithm. Cross-track gradients were removed within the APC.

The geophysical data comparisons made at this workshop were found to be remarkably good for a subset of the orbits examined. The wind determinations in both field and spot report comparisons showed about a 2 m/s standard deviation about a negative bias of less than .5 m/s. For a subset of orbits, however, good geophysical retrievals could not be made.

The distinction between "good" and "bad" revs was eventually traced to improper averaging of housekeeping temperatures used in the calibration algorithms. This deficiency in the sensor file manipulation was corrected before the processing of data for the JASIN workshop. Also for this workshop, biases for 10 T_B channels were determined to optimize retrievals for three North Pacific passes analyzed during the SMMR Mini-Workshop II.

For the JASIN workshop, wind data were retrieved for high priority JASIN revs as well as for GOASEX revs (1135, 1120, 1298) and a rev over a strong N. Atlantic storm (rev 1094). It was found that in general for wind retrievals away from land and rain by about two grid distances (about 150 km) the SMMR winds were as

accurate as could be assessed considering the errors in the surface truth. Data from both the GOASEX and JASIN areas had a standard deviation of 2 m/s. However, the wind retrievals showed a positive bias of 2.7 m/s in the JASIN area which is about 2 m/s higher than that shown in the GOASEX area (Figure 1). The positive bias in the JASIN area was also evident in comparisons of SMMR data against colocated SASS data. At least some of the scatter and bias in the JASIN comparisons has been found to be attributable to radio frequency interference (RFI) from ground sources of microwave radiation (JASIN Workshop Report, 1980).

In summary, by the time of the JASIN Workshop, much progress had been made in the evaluation of SMMR wind retrievals, but the geophysical reduction algorithms had yet to mature to the point where production and release of global geophysical data sets could begin. The comparisons had demonstrated that under certain favorable conditions, geophysical data could be retrieved with good accuracy, but a determination of what constituted favorable conditions had yet to be made.

The study reported here describes an evaluation of wind speeds derived from versions of the least-squares and regression algorithms developed after the JASIN Worshop. The specific objectives of the study were to: (1) determine the accuracy of SMMR wind retrievals in terms of the intrinsic accuracy of a baseline surface truth data set in favorable sensing conditions; (2) identify and evaluate effects which degrade the wind retrievals or introduces biases; (3) evaluate the performance of SMMR in storms with particular emphasis on effects of rain.

Evaluation Strategy

Following the JASIN workshop, a new approach based upon surface winds provided by SASS, was adopted to refine and evaluate the SMMR wind retrieval algorithm. This approach was made possible by the accuracy of SASS winds demonstrated in the JASIN SASS evaluation. The operational SASS wind retrieval algorithm was in fact developed immediately after the JASIN workshop and was used to process the entire Seasat data set (Boggs, 1981). Against the JASIN data set, the SASS 1 wind speeds were unbiased with a rms error of ±1.23 m/sec in 336 comparisons for horizontal polarization and ±1.39 m/sec in 317 comparisons for horizontal polarization. The retrieved winds appear to be unaffected by RFI clouds, cloud liquid water and rain of light intensity and to be valid to within about 50 km of land.

Comparison of SMMR and SASS winds is possible, of course, only where the sensor swaths overlap. The SASS views three separate swaths, one centered ±70 km on the nadir and the other two off nadir on the right and left sides, each extending from 200 km to 700 km from nadir. The SMMR swath is 600 km wide and extends from 50 km left of nadir to 550 km to the right of nadir. Both the regression and least squares algorithms resolve winds on grid 2, which is the resolution of the SMMR's 10.7 hz channel. SMMR grid 2 is divided into 7 columns of data 86 km wide, numbered from the nadir side of the SMMR swath.

SASS wind data used in the comparisons presented here were derived from the SASS 1 algorithm. To process the SASS data on SMMR grid 2, orthogonal pairs of SASS measurements were first converted to wind speeds (referred to 20 meter height). The average of all wind speeds for pairs whose centroids fell within the SMMR grid 2 cell was then matched with SMMR wind speed (also representative of 20 meter height).

SMMR-SASS wind comparisons played a key role in the final development of both the least squares (Wentz) and regression

(Chester) algorithms. The SMMR model function of the Wentz algorithm used SASS winds for columns 3 and 4 of grid 1 of Seasat revs 1120 and 1135. Those revs received much study in earlier workshops. Both are nighttime descending revs that extend from the Gulf of Alaska southwestward into the central North Pacific Ocean. SASS winds from rev 1135 also formed the basis of the tuning of the regression wind algorithm.

The evaluation strategy followed to achieve the objectives stated in the Introduction involved mainly two types of SMMR-SASS comparisons. In one type, SMMR and SASS winds were compared cell-by-cell for a representative sample of rev segments purposely selected to reveal the way the accuracy of SMMR winds degrades when unfavorable viewing conditions are present. The principal degrading effects examined were proximity of swath to land, and the presence of rain and high cloud liquid water in or adjacent to the swath, and for daytime revs, the effects of reflected sun in the viewing area (sunglint). In the comparisons, only three of the seven columns of SMMR data were studied in this way. The cell-by-cell comparisons are discussed relative to other sources of surface truth, such as high resolution cloud imagery, surface ship report data and conventional synoptic weather maps.

The second type of comparison involved what may be termed global statistical comparisons. Those comparisons were made for nine revs covering a much larger geographical area. The calculated statistical differences between SMMR and SASS colocated wind data were stratified by rev, column numbers, sunglint angle, and distance from rain as specified by the SMMR algorithm. The nine revs included the North Pacific revs used in algorithm development (revs 1120 and 1135); a JASIN rev extended southward to the Equator (rev 800); two revs over tropical cyclones Fico and Ella (revs 331 and 952 respectively); and four revs over an intense North Atlantic extratropical cyclone (revs 1066, 1074, 1080, 1094).

Some of the most interesting and varied data were provided by the four rev segments over the North Atlantic storm.

Detailed SMMR-SASS Comparisons in QE2 Storm

A small low pressure system moved off the New Jersey coast on September 8, 1978 and deepened explosively in the next 36 hours, causing the loss of a fishing trawler with all hands off the Grand Banks on the 9th and damage to the oceanliner Queen Elizabeth 2 on the 11th. This storm has been studied intensely. Cane and Cardone (1981) show how, despite the relatively high number of ship reports and data buoys off the U.S. East Coast, operational weather analyses and forecasts grossly underestimated the rate of deepening of the storm. Operational sea state forecasts were too low also by factors of two to four. Gyakum (1981) has used this storm to study the dynamics of explosively developing marine storms, termed "bombs" by Sanders and Gyakum (1980).

The QE 2 storm was well observed by Seasat. Particularly interesting data were returned from rev 1066 near 1200 GMT September 9, when the left side SASS swath viewed the wind field in the early stage of storm development. Rev 1080, about 24 hours later viewed the storm near maximum intensity. Revs 1093 and 1094, 24 hours after rev 1080, together covered most of the storms circulation including areas of high winds through a cloud-free atmosphere. Strongest winds measured by SASS in the storm were in rev 1080, near 1200 GMT 9/10/78. Figure 2 is reanalysis of the surface pressure field and also shows the edges of the SASS swath. The SASS winds resolved the storm center as an area of wind speeds of 10-12 m/sec with winds of 25-30 m/sec (effective 20 meter wind speeds) surrounding the center out to radial distances of about 120 n.mi. The surface wind field in revs 1093/1094, derived by detailed post-analysis of conventional data, was used to evaluate the performance of the SASS geophysical evaluation algorithm in high winds (Boggs, 1981). A comparison of SASS and ship report wind speeds within the fields of view of 1093/1094 is shown in Figure 3. Comparison of SASS and field estimates as well as the spot comparisons

(surface ship wind estimates are believed to be accurate only to within ±2.5 m/sec) support the claim the winds speeds derived from the SASS 1 algorithm have accuracies of better than 2 m/sec over at least the range 4-30 m/sec.

In the following figures which show the cell-by-cell comparisons, column 1 SMMR data are compared to SASS nadir winds estimates, which are considered to be less accurate than off-nadir SASS wind data for two reasons. First, the relationship between backscatter coefficient (σ^o) and wind speed is not as well known as the off-nadir relationship. The SASS nadir winds in fact appear to be biased high for winds above about 12 m/sec. Second, the algorithm is very sensitive to small changes in σ^o. Small decreases in σ^o due to attenuation by clouds and rain can produce large apparent increases in surface wind. Off-nadir SASS winds are generally unaffected by clouds and light to moderate rain.

Column 4 comparisons represent well the near center swath behavior, while column 7 data give an indication of edge behavior. For daytime revs in the latter half of the mission, column 7 is associated with the smallest sun angle (maximum sunglint effect).

On the figures, filled points (circles for the regression algorithm of Chester, triangles for the least squares algorithm of Wentz) represent cells at which the respective SMMR algorithm predicts rain. Land boundaries are also shown. A plot of sun angle for values less than 25° is also shown.

Rev 1066. Figure 4 shows the location of the five grid 2 blocks of SMMR data compared to SASS. They extend from 20°N to the coast of Nova Scotia. Figure 4 also shows ship reports of wind at 1200 GMT September 9, 1978, the location of fronts and cyclone centers, and a schematic depiction of the cloud field derived from visible and infrared high resolution DMSP imagery taken within one hour of the Seasat data. Block 1 lies in

generally clear air in the subtropical high pressure zone. Block 2 includes the eastern quadrant of storm Flossie which had been downgraded to a tropical depression at this time but which was undergoing reintensification. The imagery showed deep convection with imbedded towering cumulonimbus clouds in the center of the area. Block 3 and most of block 4 are in areas of generally clear to scattered cloud areas. A new cloud field is encountered near the end of block 4 and all of block 5, most of which appears from the imagery to be stratified middle and high level cloudiness. Block 5 is well east of the center of the developing QE 2 storm near 40°N, 70°W. The SASS winds retrieved to the left of nadir revealed the pattern of strong winds developing near and west of the center. East of the system and within the SMMR blocks shown overall, winds speeds did not exceed 12 m/sec.

The comparisons in this rev, shown in Figure 5, shows the following main points: (1) land effects are evident at least two grid 2 distances before the swath reaches the coast; (2) the very low sun angles in column 7 especially cause large positive biases in both algorithms, which begin to show up also in column 4 as the sun angle decreases below 20°; (3) in column 1 the Chester winds are biased low by about 1 m/sec and the Wentz winds high by 1 m/sec (away from rain areas) in blocks 1, 2 and 3, but both algorithms agree in the clear air in block 4; (4) the wind estimates from both algorithms are degraded in the area of convection (and associated high cloud liquid water and rain rates) that extends northeastward across block 2, though the Wentz algorithm, especially in column 4, appears to be more transparent to the rain; gaps in the SASS data do not allow a good determination of algorithm behavior in the rain area in blocks 4/5 associated with the stratiform cloud field, though effects appear to be much smaller there.

Rev 1074. This revolution segment viewed the western Atlantic between the U.S. East Coast and the QE 2 storm. At the

time of the revolution, the storm center is located near 40°N, 55°W, well east of the SMMR swath. However, the rain shield around the cyclone extends westward to cover the northeast corner of block 1, as shown in Figure 6. Figure 6 also shows the available ship reports, the outline of solid cloud cover shown in the DMSP infrared image and the outline of land masses.

The analysis of several DMSP images (e.g., Figure 7) and the ship reports allowed the identification of areas of: (1) continuous precipitation from the thick stratified cloud shield in the northeast corner of block 1; (2) light showery precipitation from the relatively shallow maritime convection in the polar air stream behind the cyclone, which occupies most of blocks 1 and 2; and (3) cumulonimbus towers in the northeast corner of block 3, probably causing small areas of heavy showery precipitation there.

The column 1 (Figure 8) wind comparisons show the over-specification of surface winds by the SASS nadir winds in the first two blocks, where both SMMR algorithms provide winds in close agreement with surface data. In blocks 1 and 2, the SASS nadir data, because of the small footprint size compared to the SMMR grid 2 cell size, respond to the small rain shower cells more sensitively than the SMMR, though the Wentz algorithm occasionally specified rain in that area.

The wind comparisons are generally good in column 4 and 7 (Figure 8), except for a slight positive bias in blocks 1 and 2 which is increased in column 7. The source of this positive bias is not entirely clear, though proximity of the right-hand side of blocks 1 and 2 to the U.S. East Coast suggest that land contamination is present. Spurious wind responses in the beginning of block 3, columns 1 and 4 especially, are related to the proximity of the area of cumulonimbus towers of high cloud liquid content.

Rev 1080. The revolution extended from the sub tropics northward to near the center of the QE 2 storm when the storm was at its maximum intensity. Figure 2 is a reanalysis of the surface pressure field. Figure 9 shows the location of the SMMR blocks compared. The cloud imagery (Figure 10) shows considerable cloudiness of varying coverage between blocks 3 and 5 with embedded areas of dense overcast suggesting precipation. Both SMMR algorithm specify rain in parts of blocks 3, 4 and 5.

The comparisons in this rev (Figures 11 and 12) show the variability in the response of the algorithm in rain. For example, in the first three cells of block 3, both algorithms track similarly through the rain system in column 1 but differently in colums 4. In column 1, the SASS winds are biased high in blocks 4 and 5 for reasons discussed above when both algorithms provide winds in good agreement with field analyses. In column 4, both algorithms provide reasonably good winds in the area of winds above 20 m/sec, despite the indication of rain and sun angles of about 15°. Sun angles are generally less than 10° in column 7where the Wentz winds exhibit more bias than the Chester winds, but above about 20 m/sec, both algorithms track the SASS winds well despite the indicated presence of rain.

Rev 1094. This revolution viewed the QE2 storm on the same day that the ship sustained damage in 50-foot waves and 60-knot winds. The area of SMMR-SASS overlap of Rev 1094 viewed the western side of the storm circulation.

Figure 13 shows the location of the storm center, the QE2, other ship reports, and the location of the five blocks of SMMR data compared to SASS. The map also shows the location of a frontal band of cloudiness (shown on GOES imagery) intersecting block 1. Ship reports in the frontal cloud band reported showery precipitation along with a narrow zone of increased wind speeds. The northern blocks included part of the very strong circulation about the storm, with winds up to about 25 m/sec, viewed through a mainly rain-free atmosphere.

The SMMR-SASS comparisons for columns 1 and 4 are shown in Figure 14 with the column 7 comparisons in Figure 15.

Column 1 comparisons reflect the frontal band in block 1 with both algorithms detecting rain and the SASS nadir winds overspecifying the surface winds. Surface truth data suggest peak winds of about 12-14 m/sec in the frontal band. Between the front and the Newfoundland coast, agreement is good between SASS and SMMR winds except where the surface winds increase to above 12 m/sec and the SASS nadir winds begin to overestimate.

Column 4 comparisons are excellent north of the frontal band except where the column parallels the Newfoundland and Labrador coasts (within two grid 2 cell distances). Both SMMR algorithms overestimate the surface winds in the frontal band substantially. South of the front in the rain-free atmosphere, both algorithms are biased high in the area of 4-6 m/sec SASS winds. This bias appears to be a result of sunglint, which apparently begins in light winds at sun angles as high as 15°.

The sunglint contamination is even more evident in the column 7 comparisons. However, as shown also in the comparisons of rev 1080, the degree of sunglint contamination appears to decrease with increasing surface wind (e.g., blocks 3 and 4) even for low sun angles. The performance of the SMMR in blocks 3, 4 and 5 is striking, suggesting wind speed sensitivity in high winds comparable to the SASS.

This and other revolutions examined suggest that the user might be able to successfully correct the released SMMR GDR data for sungling effects through an empirical algorithm which considers gointly sun angle and wind speed. A recent theoretical model (Swift, 1980) might be used to guide such an algorithm.

Comparisons in an Extended Rev Segment

Figure 6 shows the column 4 SMMR-SASS comparison for an extended segment of rev 800, which begins near 69°N in the northeast North Atlantic, crosses the JASIN area in block 3, the Azores in block 7, and terminates in the equatorial Atlantic near 5°N. This was a southbound, nighttime orbit, which occurred during the JASIN experiment.

The revolution crosses rain areas at the end of block 2, the beginning of block 5 (near 50°N), and in the intertropical convergence zone at about 7°N. The behavior of the wind retrieval in and near rain is somewhat different in the two algorithms, but most of the revolution is indicated to be rain-free.

Both algorithms return reasonable winds compared to the SASS, in the JASIN area. Just north of the JASIN area, Wentz winds are low and Chester winds high compared to the SASS, where the Wentz algorithm detects rain. In addition, detailed prior sturies of this revolution have detected RFI both near the JASIN area and over the Azores, where both algorithms depart from the SASS.

This segment reveals the tendency for the SMMR-SASS differences to be spatially coherent on scales of the order of the block dimension. Note, for example, the excellent tracking in blocks 6, 10, 11, and 12 and the systematic differences in blocks 2 and 4. The cause of such differences is not known.

Overall Statistical Summaries of Filtered Data

QE2 Data. The cell-by-cell comparisons in the QE2 revs clearly demonstrate the major factors which degrade the performance of the SMMR wind algorithms: land contamination, rain, sun glitter. In this section, we summarize the performance of the Chester algorithm (which was used to process the entire data set). in the most favorable viewing conditions applying simple filters to the data to eliminate most, but not all, of the degrading effects of land, rain and sun glitter.

The filter applied to eliminate most of the sun glitter consisted of excluding comparisons if the sun angle is less than 10° or if the sun angle is less than 15° and the wind speed is less than 15 m/sec. To filter rain, comparisons were excluded at or adjacent to cells at which the SMMR indicates that rain is present. The rain filter implicitly eliminated near land cells, since brightness temperatures of land trigger a positive response from the rain algorithm. The influence of land outside the swath however is more difficult to filter. Rev 1074, which paralells the U.S. East Coast appears to have been affected by land, as indicated by an increasing negative bias (SMMR-SASS) in both algorithms going from columns 4 to 7. This suggests that even at distances of 500 km, the antenna pattern correction algorithm overcompensates for the hot thermal emissions of land entering the antenna site lobes (see also Wentz et al., 1982). For Rev 1074, therefore, comparisons were included for columns 6 and 7. For all revs, columns 1 and 2 were also excluded, so that no nadir SASS data would be used in the comparisons.

Figure 17 is a scatter plot of the filtered SMMR-SASS comparisons for the four QE2 revs. Different symbols are used for each rev. The data may be characterized as those pertaining to "favorable" viewing conditions of active mid-latitude wind fields. There remains a correlation of bias with Rev; particularly evident is the low bias (SMMR-SASS) of 1074 suggesting

residual contamination by land. Over the 140 points, the scatter is under 2 m/sec, about a bias of 1 m/sec. The sensitivity of the passive system, moreover, appears to be comparable to the active system.

Global Statistics. The final three figures summarize all of the SMMR-SASS comparisons to date. Figure 18 shows the comparisons plotted against column for each of the nine revolutions. The comparisons are screened to eliminate points that are less than two cells away from rain (land shows up as rain) as well as points with a sun-glint angle less than 10°. The results for columns 1 and 2 have not been connected to the results for the other columns because of the previously mentioned problems with the nadir SASS winds and thus will be ignored. Note that almost all of the comparisons have a scatter of less than 2 m/sec, with biases independent of column, and that they fall within 0-2 m/sec. The exceptions are (1) the Wentz comparisons for Revs 952, 1066, and 1080, where the algorithm is probably showing a sensitivity to sunglint angles just above the 10° cutoff used; and (2) the comparisons for Rev 1074, which are probably contaminated by land.

Figure 19 explores the sunglint effect further by plotting comparisons screened for rain versus sunglint angle. Revs 1066 and 1084 clearly show the increases in the SMMR-retrieved wind with smaller sun angles. The curve for Rev 1080 is different because the actual wind speed in that pass increases where the sun angle is less than 10°, which decreases the effect.

The effect of distance from rain is explored in Figure 20. Again, sun angles less than 10° have been screened out of the data. Because of the presence of land also causes the algorithms to report rain, it was impossible to untangle the two effects here. As noted before, the Chester algorithm is definitely biased high whenever a cell reports rain, but is apparantly unbiased when rain is one or more cells away. Both algorithms show a large scatter at and near rain cells. In order to obtain

a scatter less than 2 m/sec, the comparisons must be restricted to those cells greater than two cells away from rain.

From all of these comparisons, when account is made for rain and sunglint effects, we conclude that the SMMR-SASS scatter is less than 2 m/sec about a bias of 1-2 m/sec.

Summary and Conclusions

The first geophysical data processed from SMMR provided encouraging though preliminary evidence that ultimately the design specification for accuracy of wind speed determinations from SMMR could be demonstrated. Geophysical evaluation of the data was limited in the early stages by problems associated mainly with the calculation of unbiased brightness temperatures. As the data reduction problems were overcome, attention was focussed on the refinement of the SMMR geophysical reduction algorithms.

It would found to be more difficult to produce a definitive surface truth data set for evaluation of SMMR derived winds than for the SASS because most of the data buoys relied upon for high quality surface wind data are very close to land, where SMMR retrievals are contaminated by land effects. Early verification of SMMR wind data therefore relied upon data from conventional surface ship reports and marine surface wind field analyses. The error in such surface truth sources is generally more than ±2 m/sec.

Final tuning of the SMMR algorithms made use of SASS wind data, whose accuracy had been demonstrated previously against high quality surface data. This report presents an extensive comparison of SMMR and SASS wind estimates covering both favorable and unfavorable viewing conditions.

SMMR data from favorable conditions appear to easily meet design specifications of accuracy, and provide surface wind speed measurements accurate to better than ±2 m/sec about a bias of about 1 m/sec over the range of wind speeds 0-25 m/sec. Higher wind speeds were not measured in favorable conditions in the data set examined. Favorable data means that the area viewed by the SMMR is at least 500 km away from land, at least 180 km away from rain and that the local sun glint angle is

greater than about 20°, though in surface winds greater than about 15 m/sec, errors in SMMR derived surface wind speeds appear to be small even for sun angles of less than 10°.

Unfavorable viewing conditions therefore may be defined as proximity to land, rain or the presence of sunglint. It appears that SMMR data contaminated by reflected solar energy may be correctable, though the GDR data released has not been so corrected. Retrieval of accurate wind speeds in data close to land or rain will be more difficult to achieve.

References

Brown, R.A., V.J. Cardone, J. Hawkins, J.E. Overland, W.J. Pierson, S. Peterherych, J.C. Wilkerson, P.M. Woiceshyn, M. Wurtele. 1982: Surface wind analysis for Seasat. To appear in first Seasat Special Issue of J. of Geophys. Res.

Boggs, D.H., 1981: The Seasat scatterometer model function: The genesis of SASS I. JPL Report 622-230. Jet Propulsion Laboratory.

Cane, M.A., and V.J. Cardone, 1981: The potential impact of scatterometry on oceanography. In: Oceanography from Space, J.F.R. Gower, ed. Plenum Publishing Company.

Gyakum, J.R., 1981: On the nature of explosively developing cyclones in the Northern Hemisphere Extratropical Atmosphere. Ph.D. Thesis. Mass Inst. of Techn. Department of Meteorology.

Jet Propulsion Laboratory, 1980: Seasat-JASIN Workshop Report. JPL Publication 80-82, Volume 1. Jet Propulsion Laboratory, Pasadena, CA.

Lipes, R.G., R.L. Bernstein, V.J. Cardone, K.B. Katsaros, E.G. Njoku, A.L. Riley, D.B. Ross, C.T. Swift, F.J. Wentz, 1979: Seasat Scanning multichannel microwave Radiometer: Results of the Gulf of Alaska workshop. Science, 204, 1415-1417.

Sanders, F. and J.R. Gyakum, 1980: Synoptic dynamic climatology of the "bomb." Monthly Weather Review, 108, 1589-1605.

List of Figures

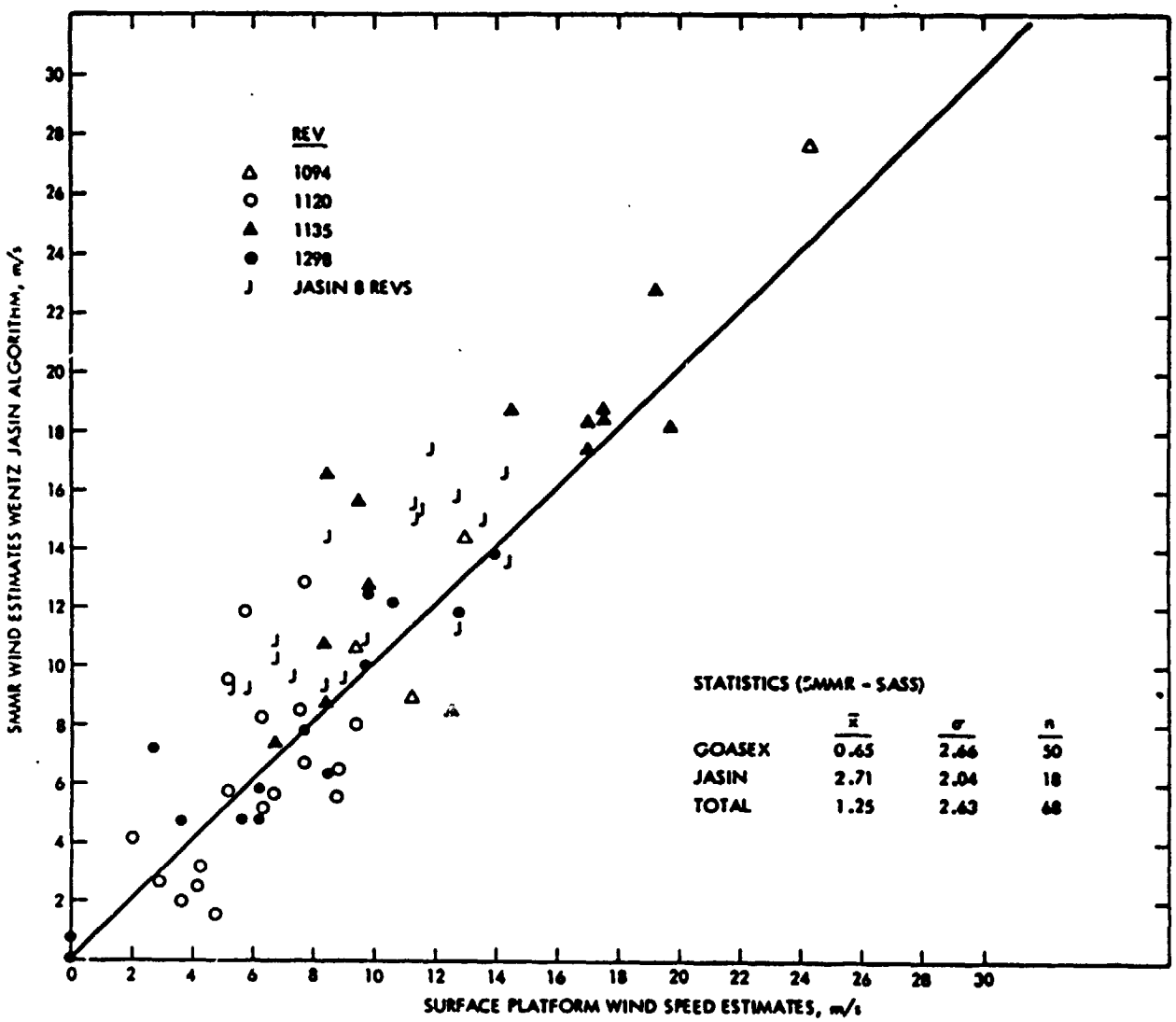

Wentz Wind Speed Comparisons - GOASEX Revolutions, Spot Reports

Figure 1

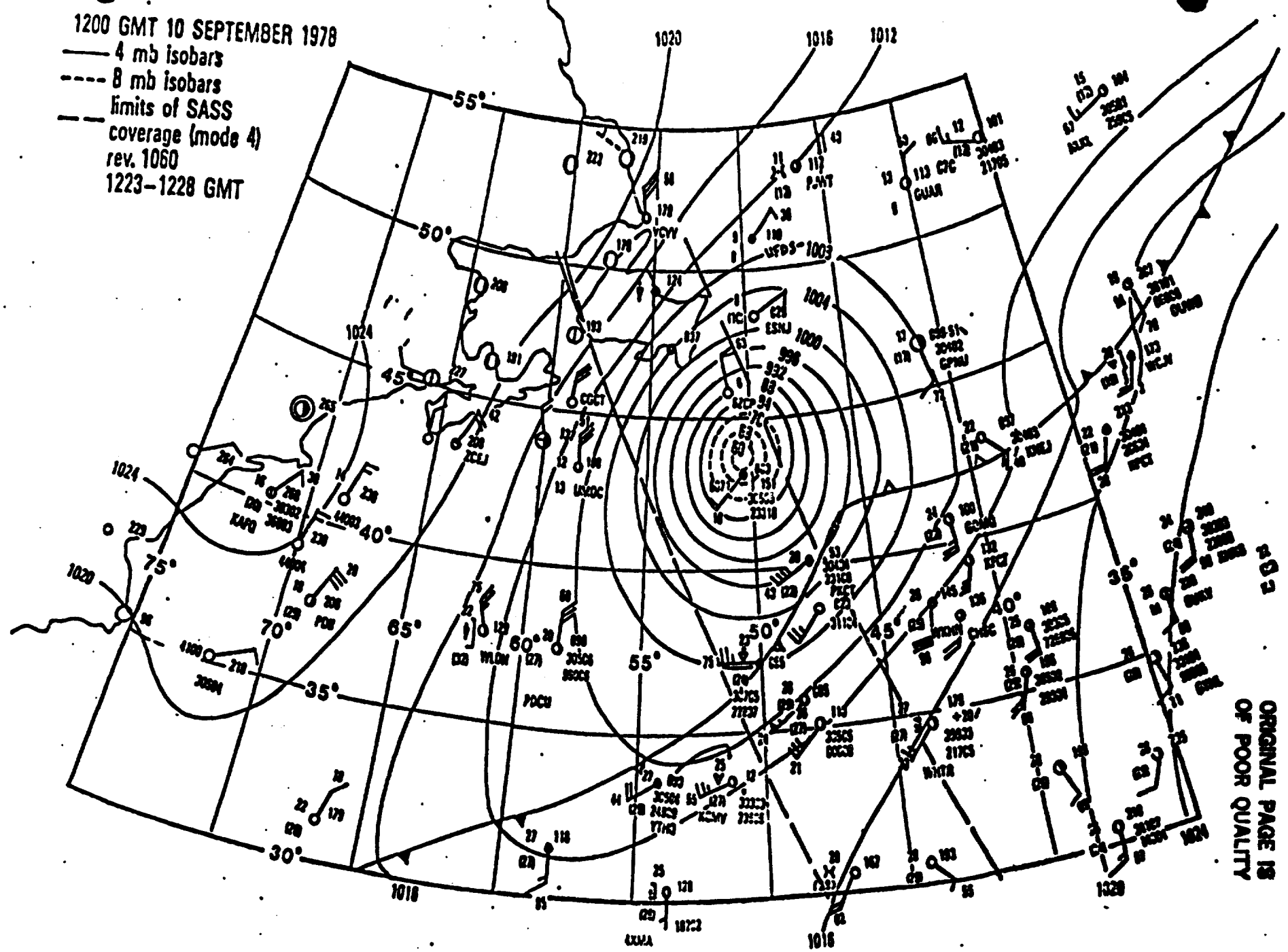

Figure 2 Reanalysis of surface pressure, incorporating additional data, (Cane & Cardone, 1981) for 12 GMT Sept. 10, 1978. SASS swath indicated.

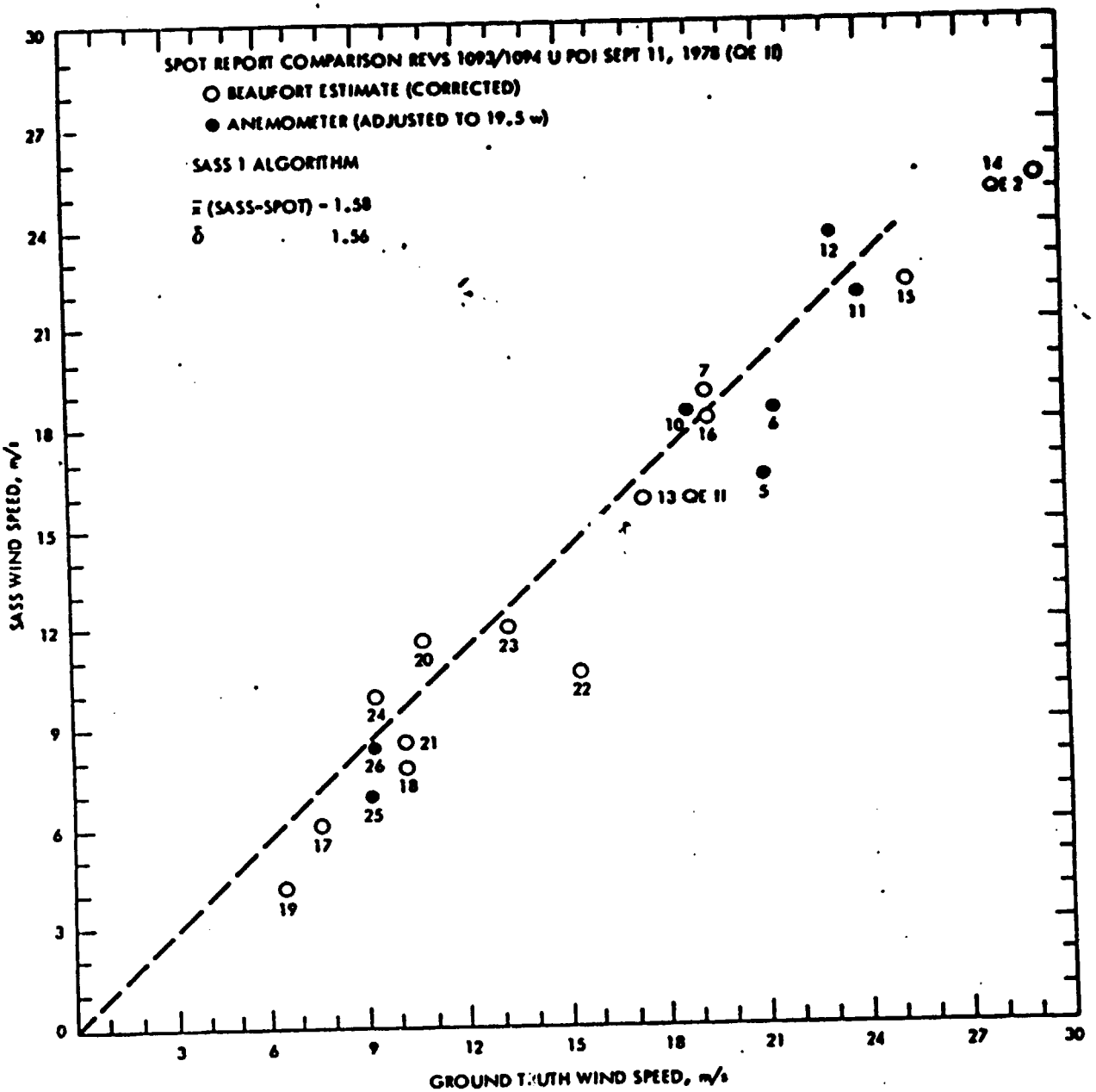

Figure 3

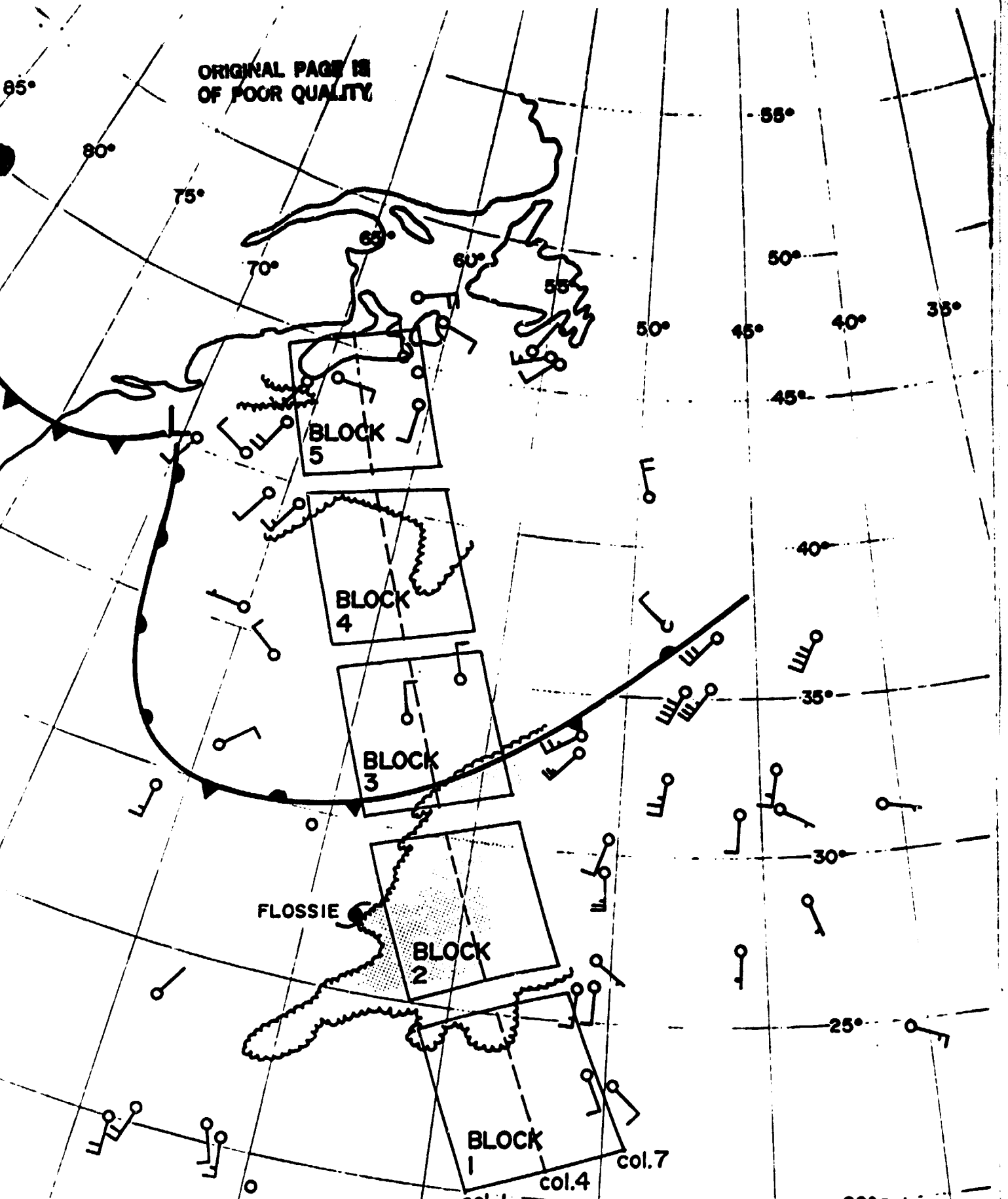

Figure 4

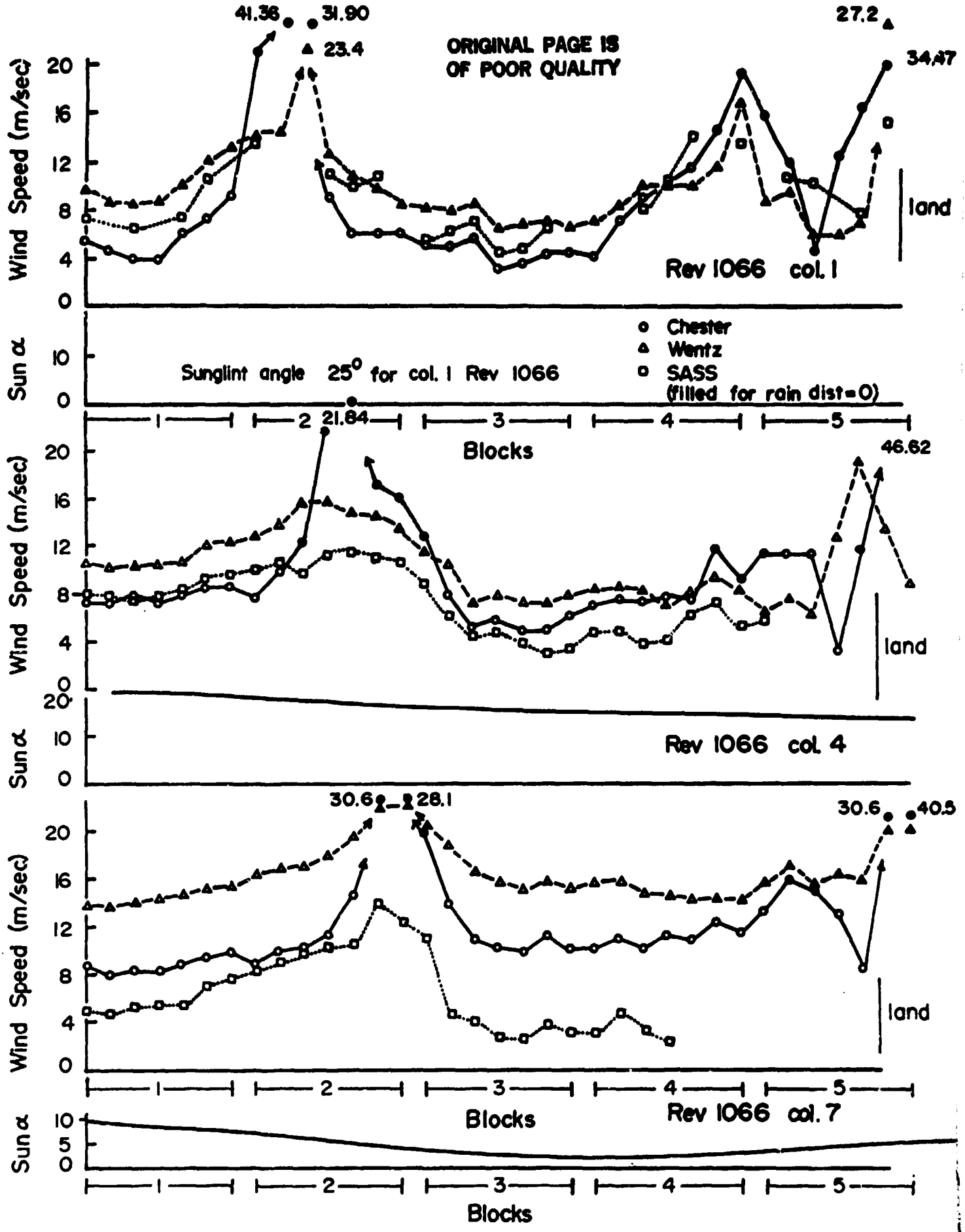
41.36
31.90
23.4
27.2
34.47
ORIGINAL PAGE IS
OF POOR QUALITY
Wind Speed (m/sec)
land
Rev 1066 col. 1
Sun α
Sunglint angle 25° for col. 1 Rev 1066
Chester
Wentz
SASS
(filled for rain dist=0)
21.84
Blocks
46.62
Rev 1066 col. 4
30.6
28.1
30.6
40.5
Rev 1066 col. 7

Figure 5

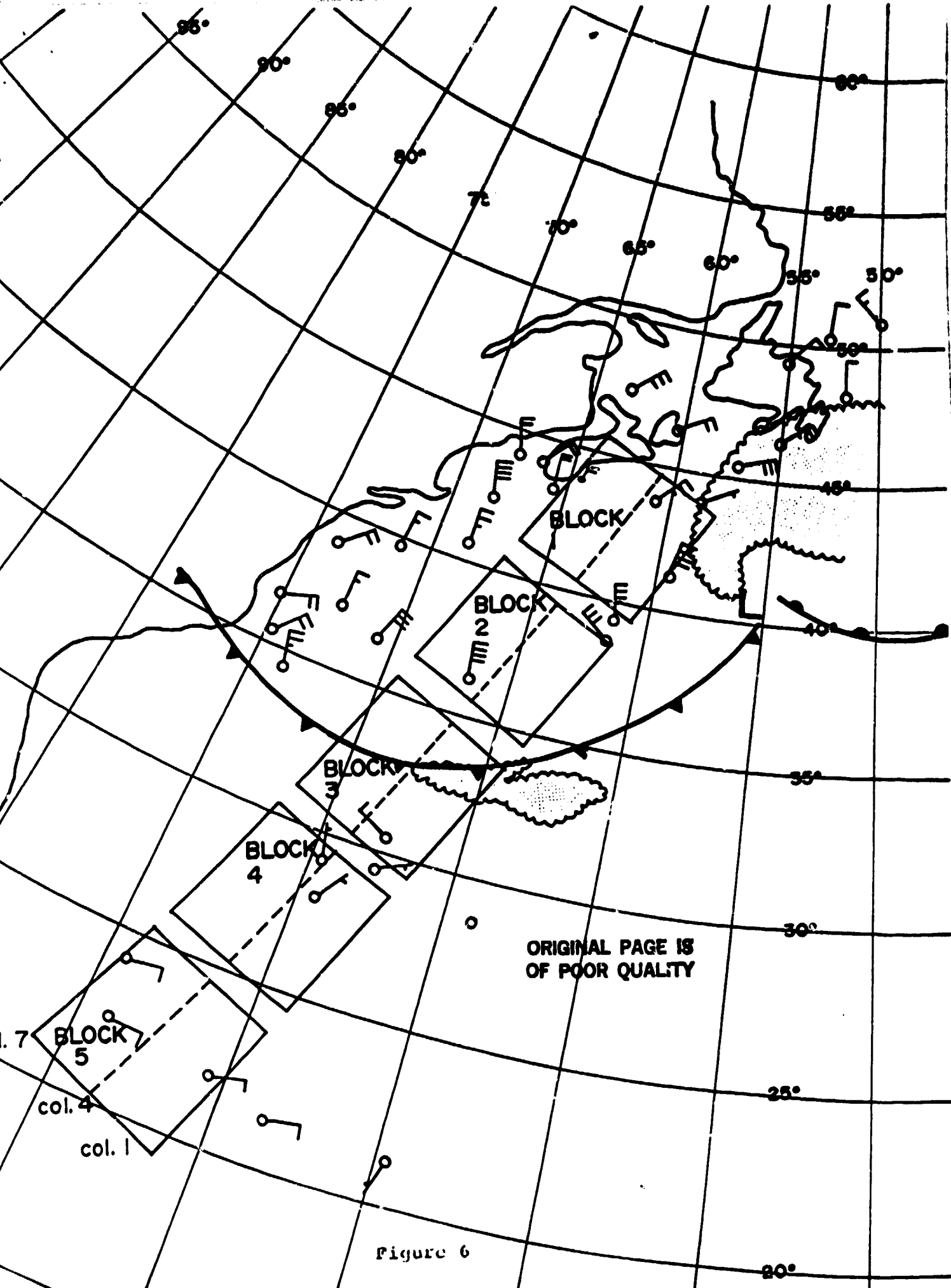
BLOCK
BLOCK 2
BLOCK 3
BLOCK 4
BLOCK 5
col. 7
col. 4
col. 1
ORIGINAL PAGE IS
OF POOR QUALITY

Figure 6

Figure 7

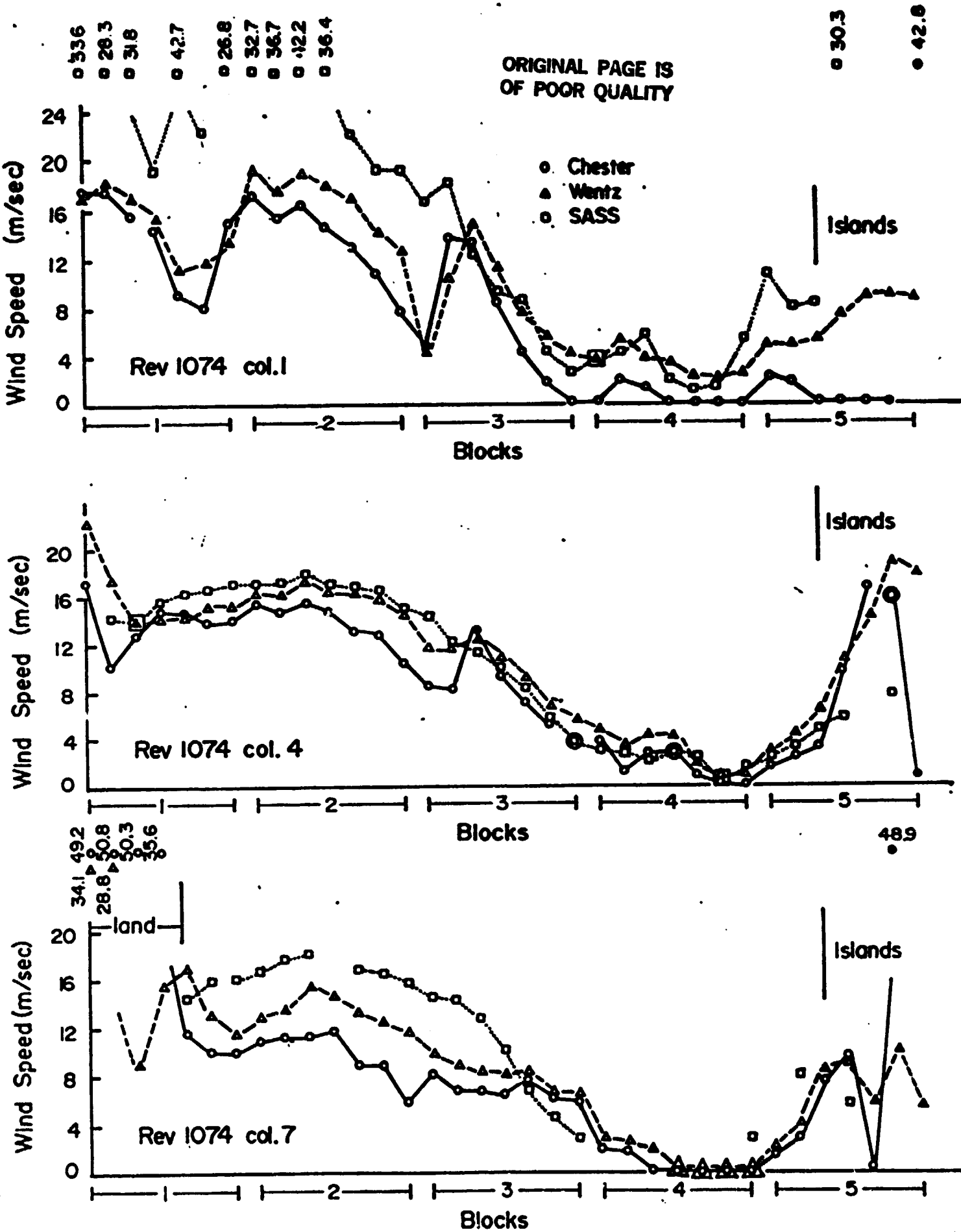

Figure 8

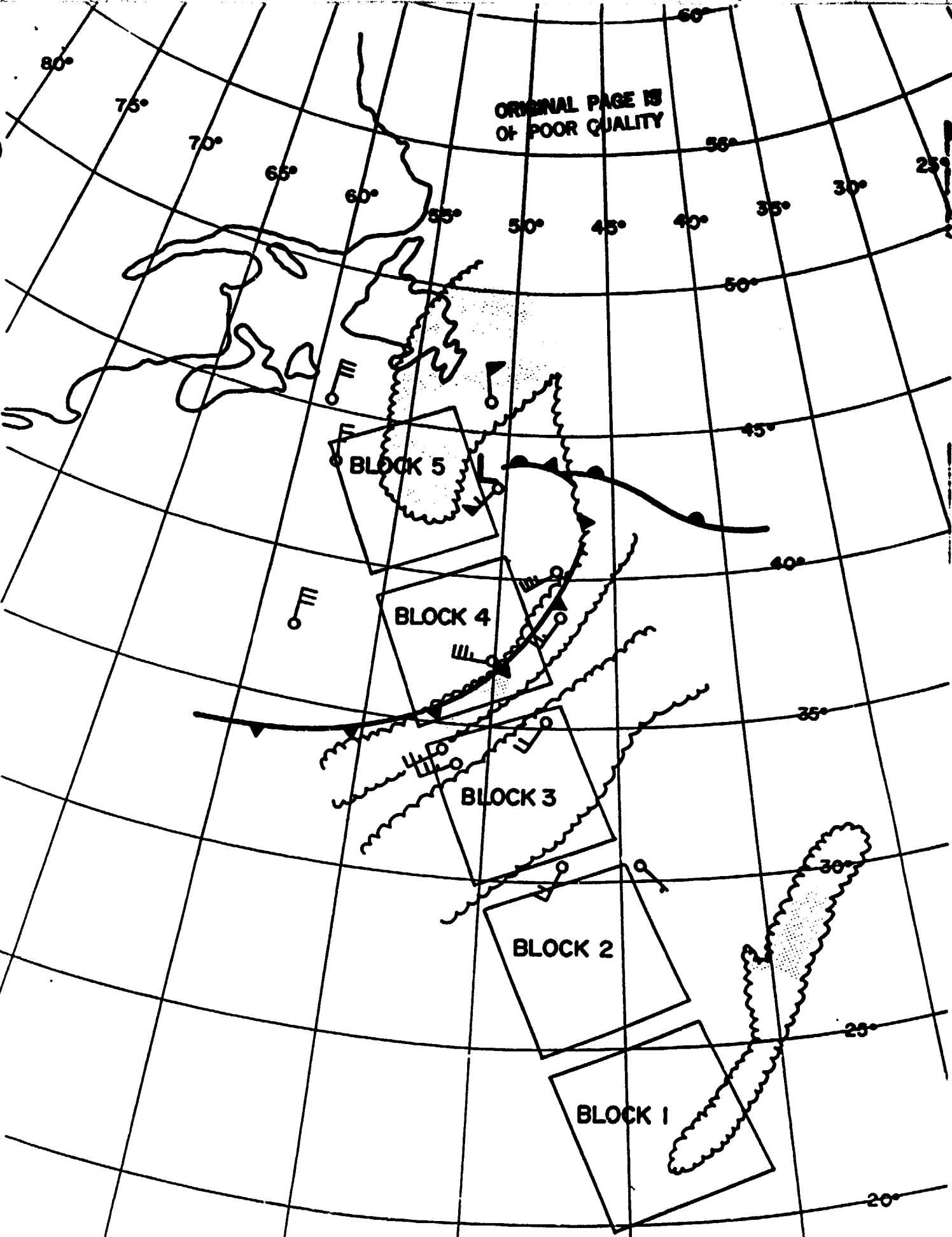
ORIGINAL PAGE IS
OF POOR QUALITY
BLOCK 5
BLOCK 4
BLOCK 3
BLOCK 2
BLOCK 1

Figure 9

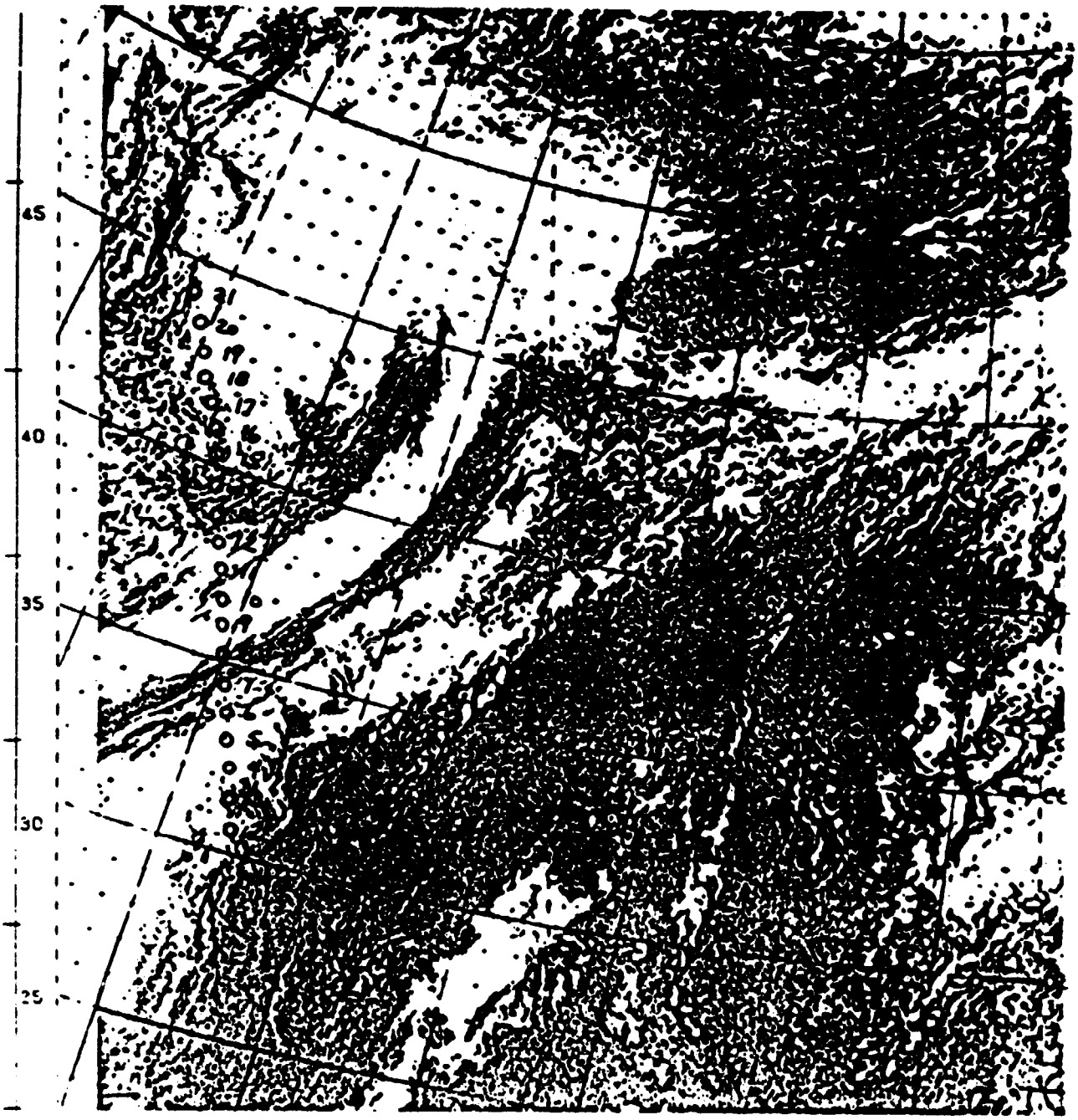

Figure 10 Rev 1080 SMMR Grid 2, Column 4, Cell Locations Plotted on a DMSP Visible Image

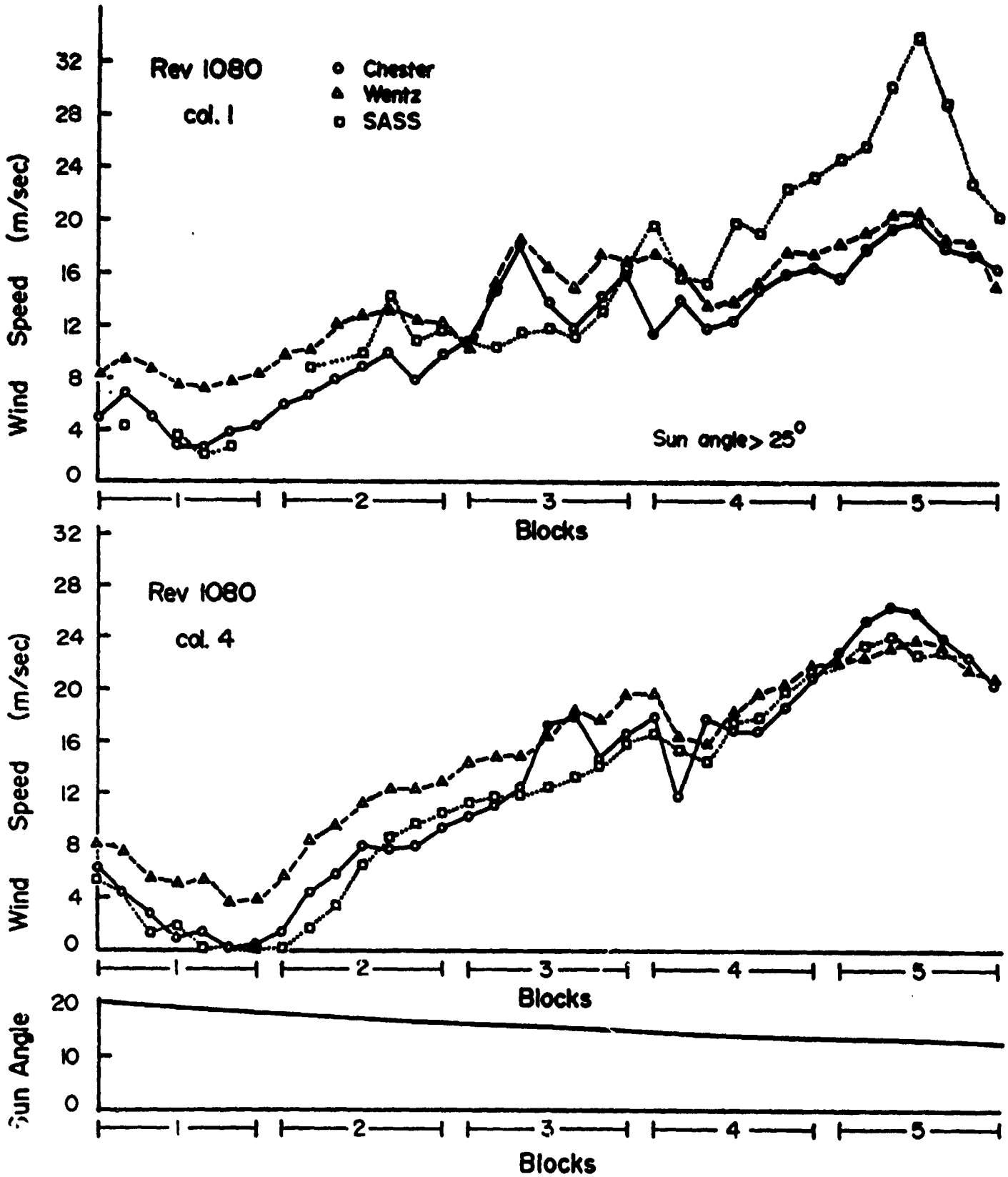

Figure 11

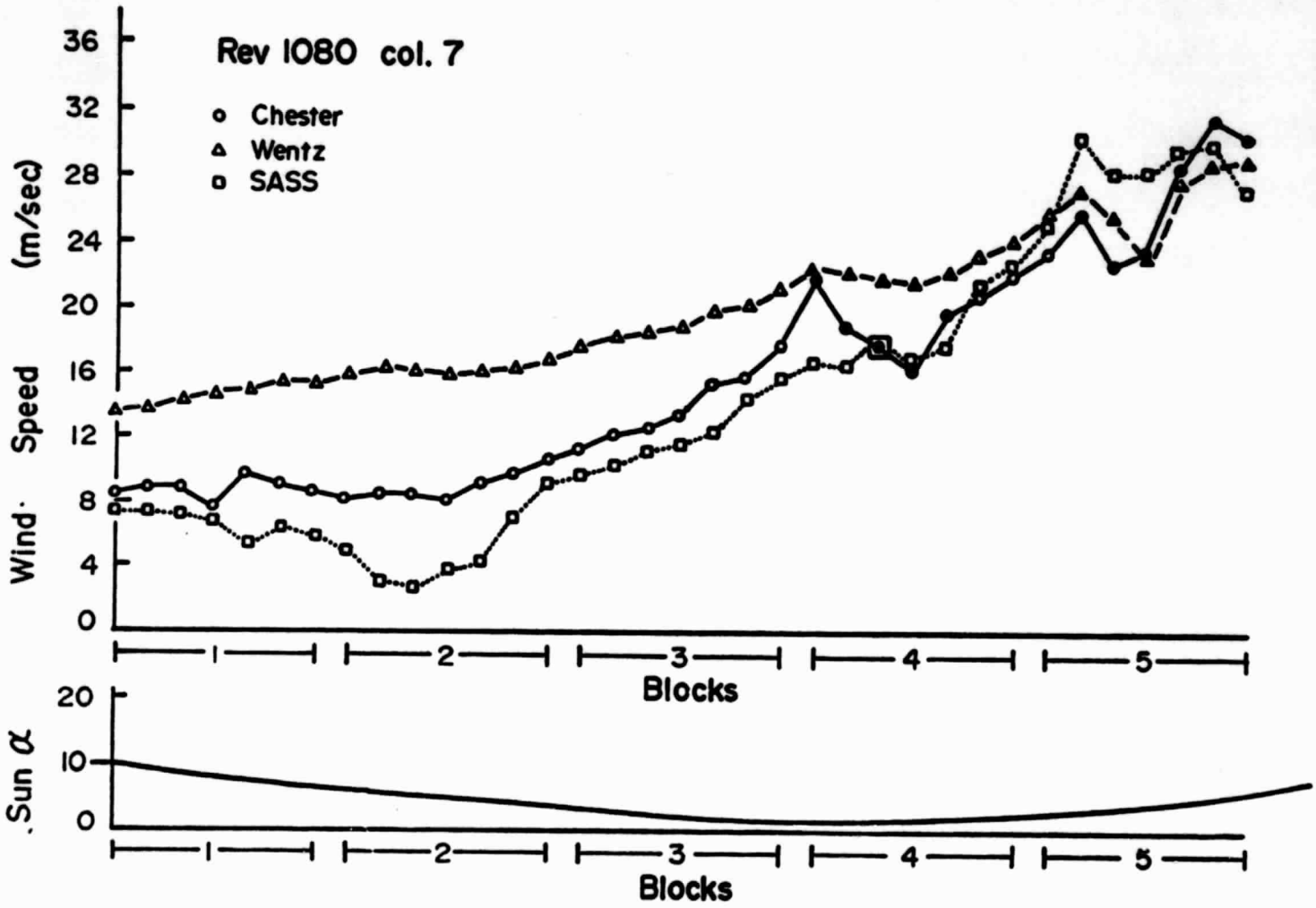

Figure 12

Figure 13

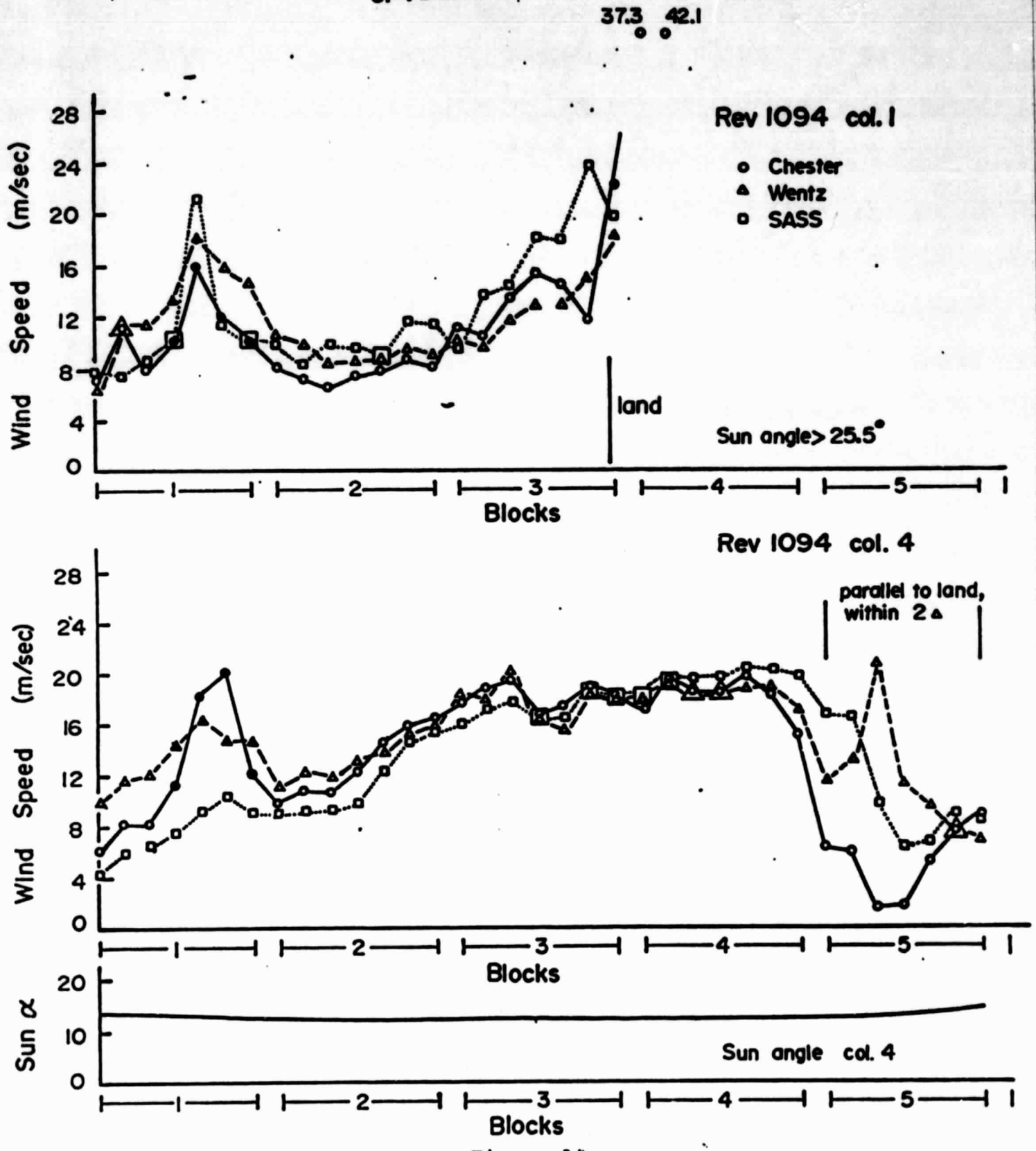

Figure 14

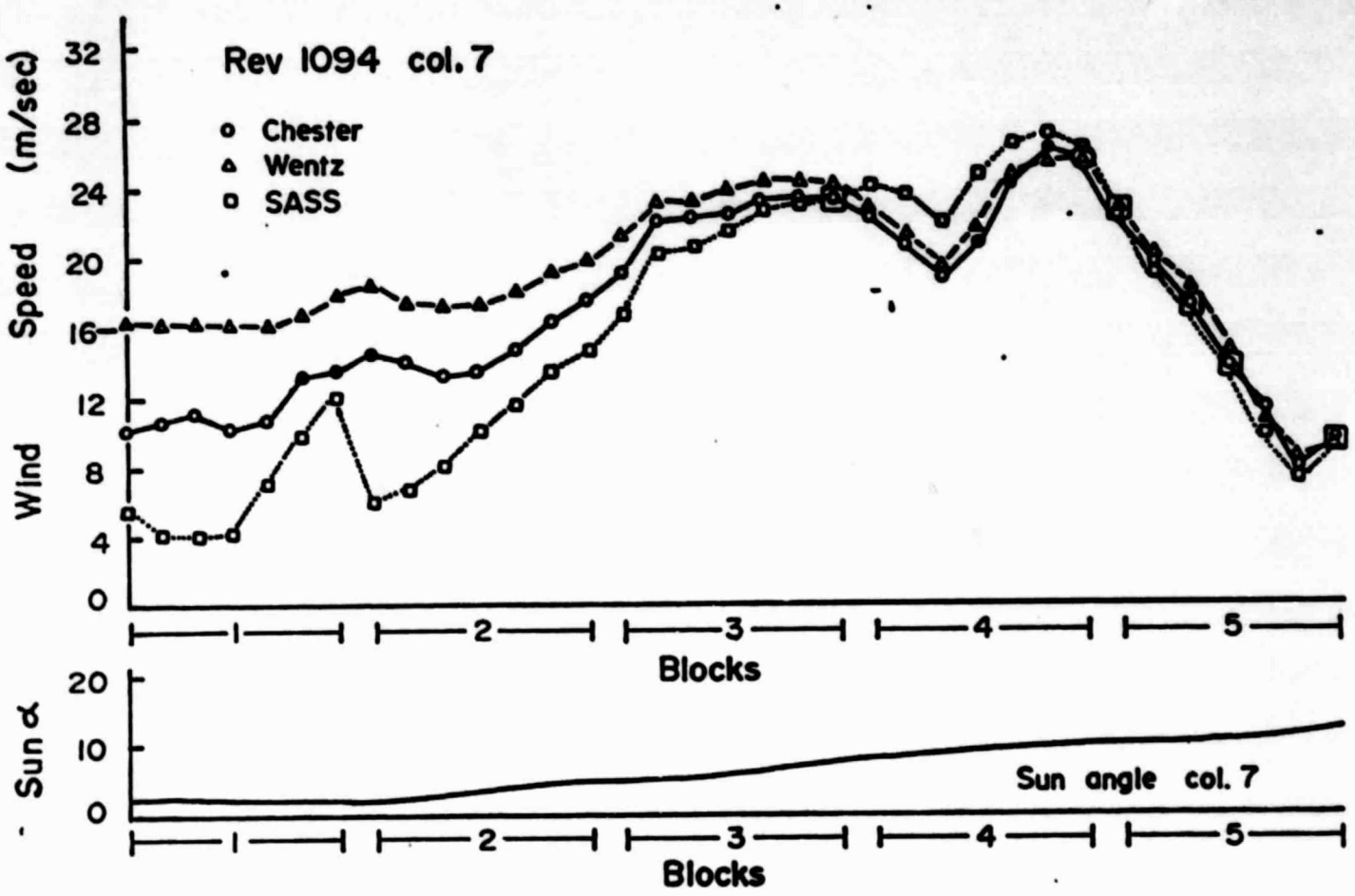

Figure 15

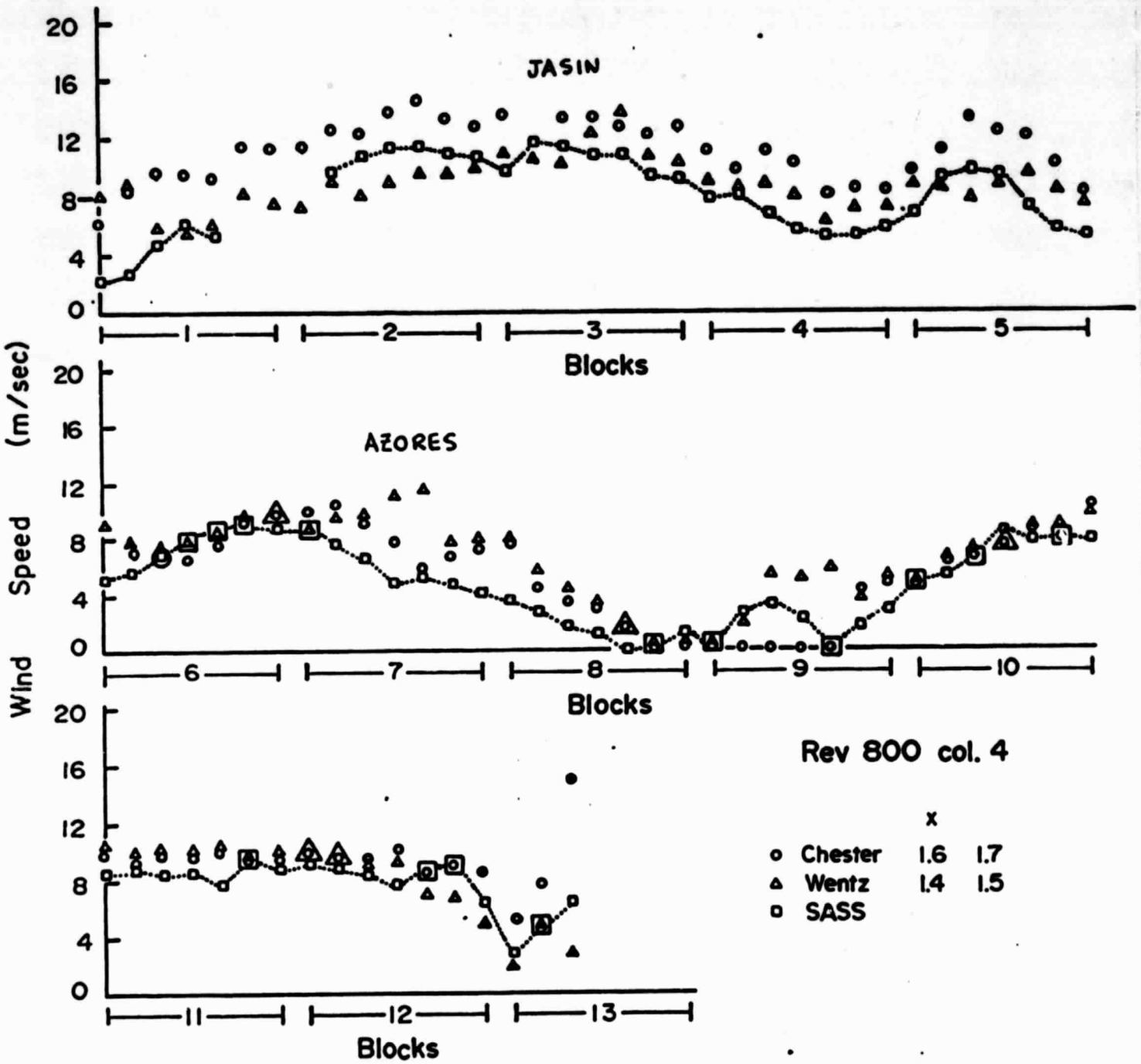

Figure 16

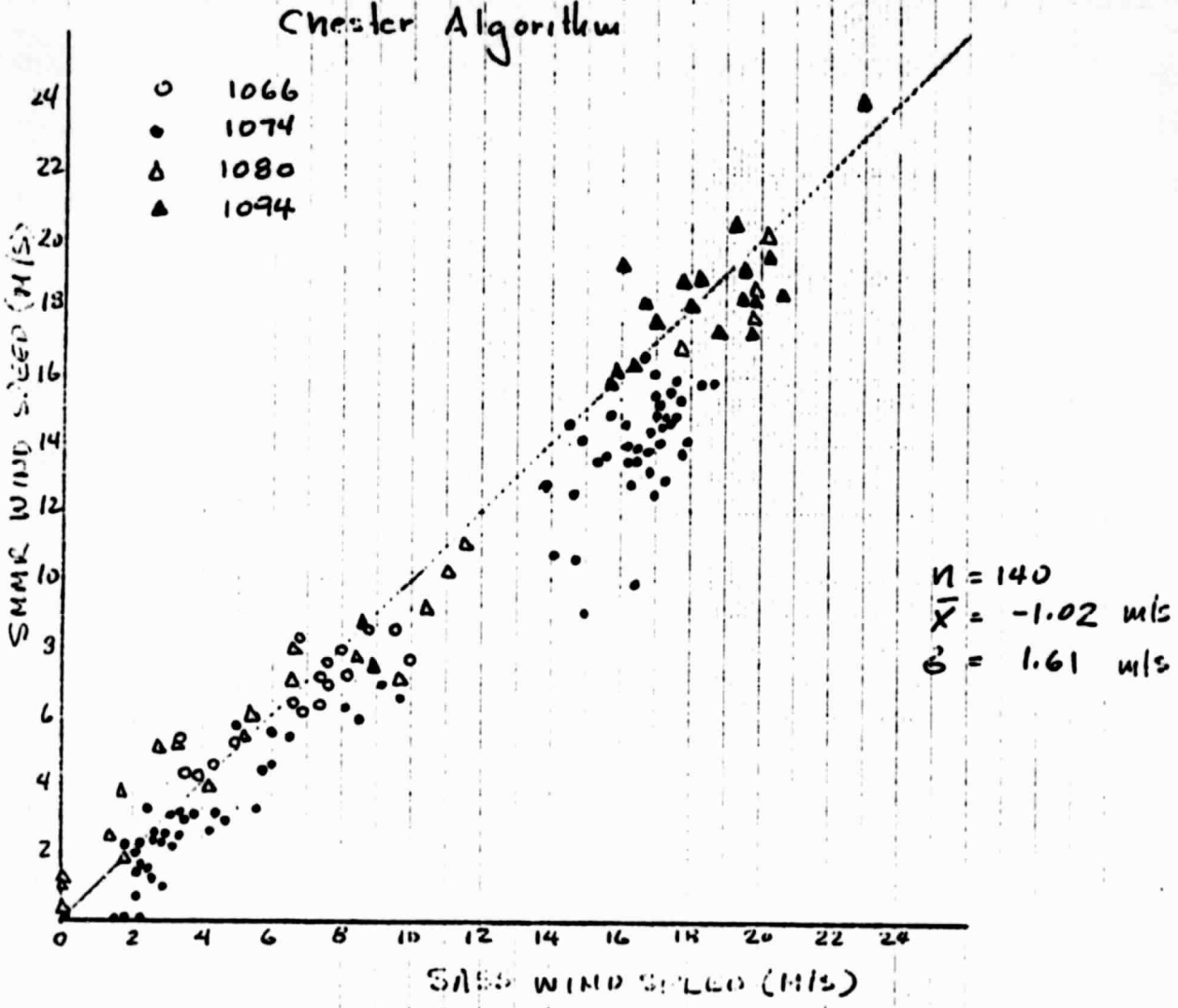

Figure 17

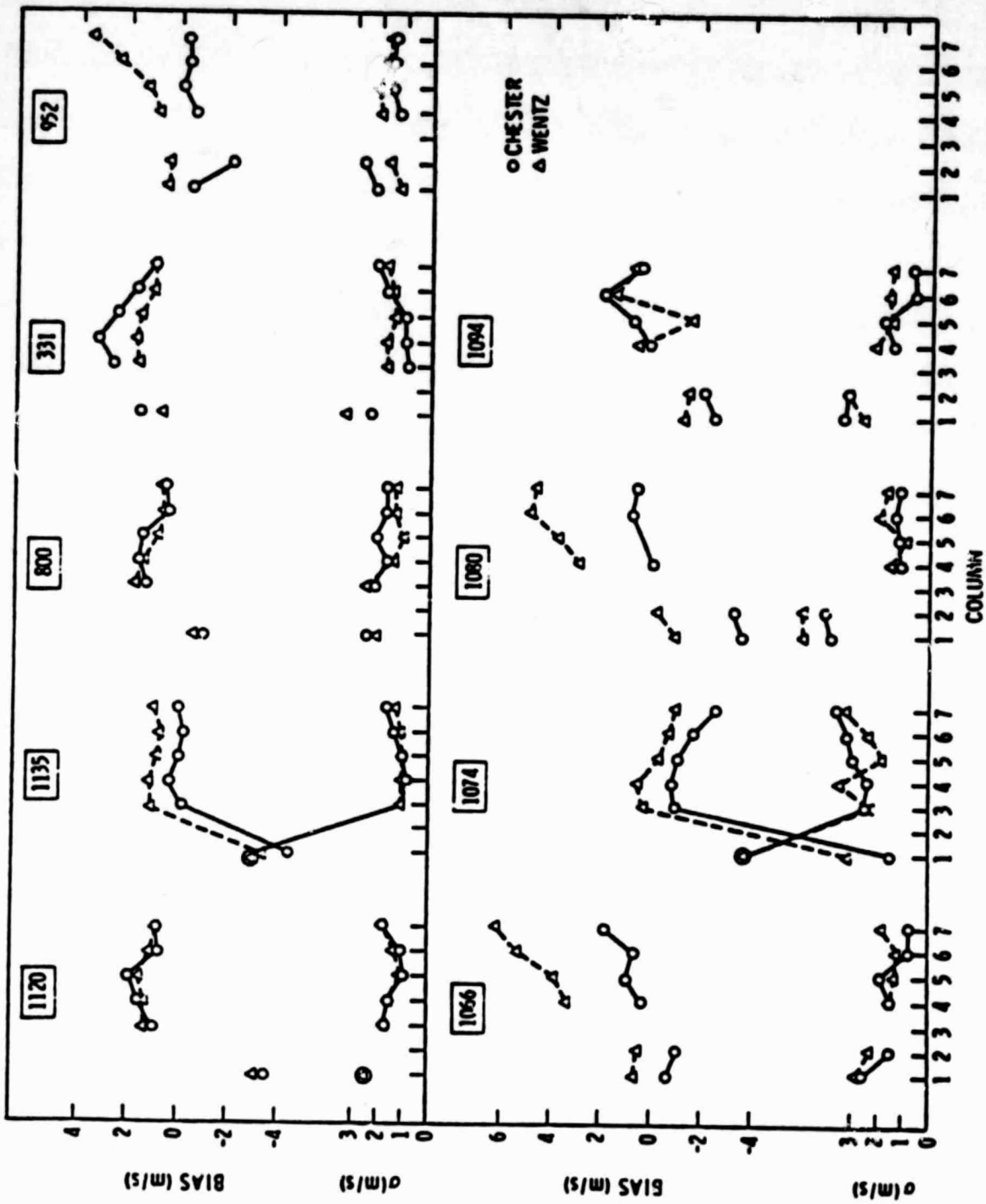

Figure SMMR-SASS versus Column Position

Figure 18

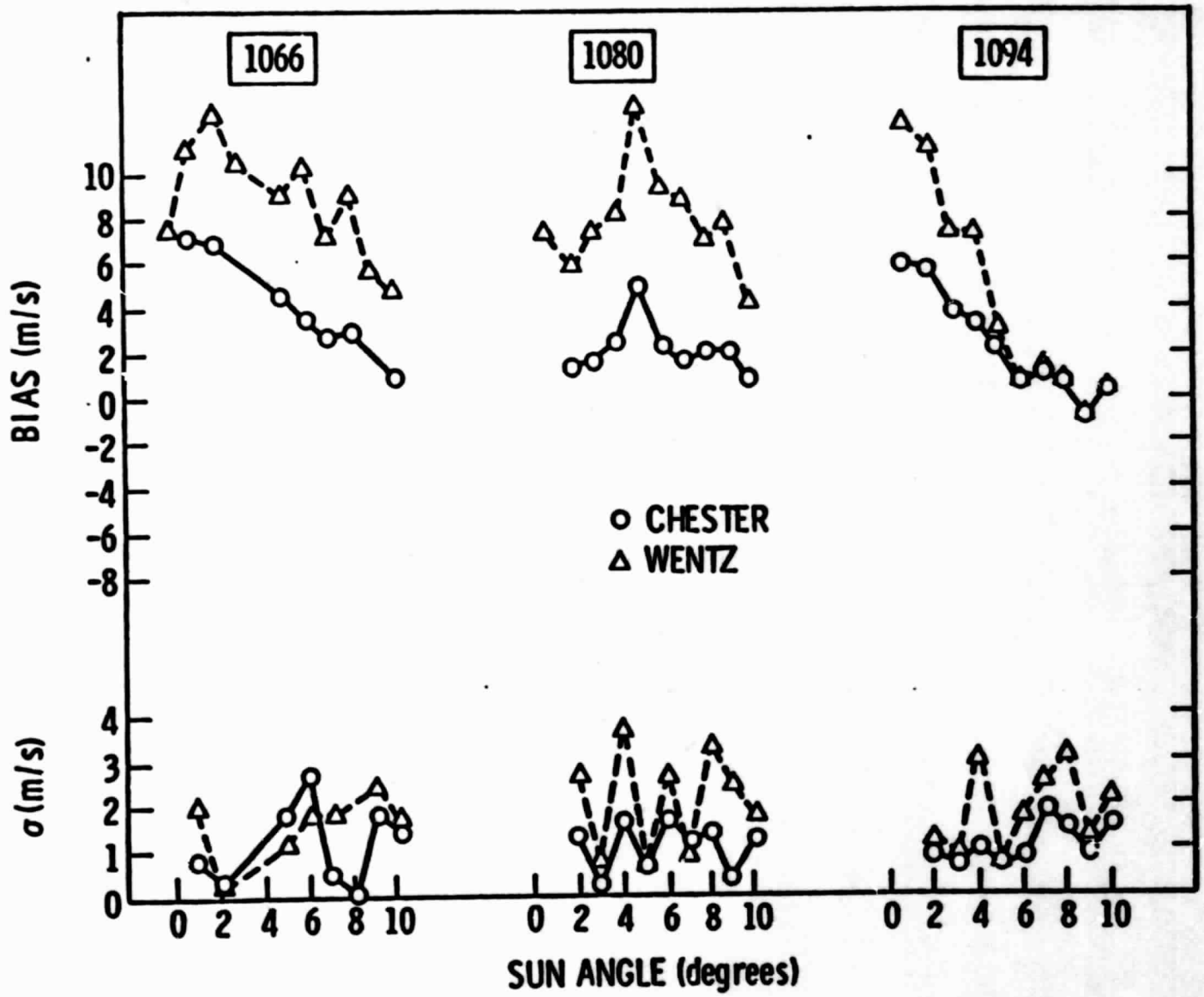

Figure 13

Figure SMMR-SASS versus Sun Angle

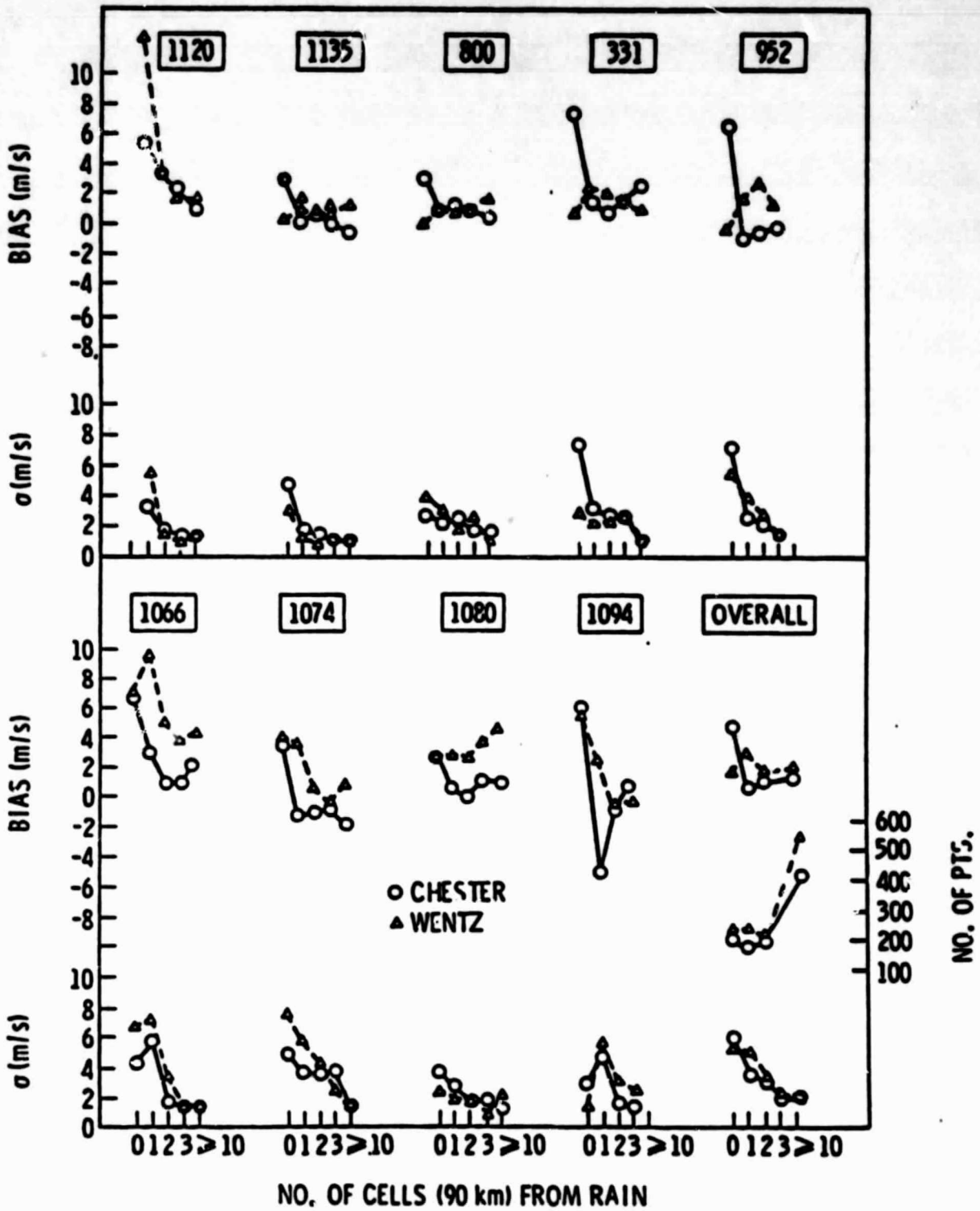

Figure 20 SMMR-SASS versus Distance From Rain